Volume 32
Number 1
January 6, 1993

Inorganic Chemistry

Articles

Reactivity and Acidity of Li in $LiAlO_2$ Phases

Richard Dronskowski[†]

Department of Chemistry and Materials Science Center, Cornell University, Ithaca, New York 14853-1301

Received March 26, 1992

With the help of semiempirical electronic structure calculations, we seek to understand why solid α-$LiAlO_2$ exchanges Li^+ with H^+ while in contact with molten benzoic acid but γ-$LiAlO_2$ does not. After critically examining the structural data for $LiAlO_2$ modifications, we calculate the binding and both the static and dynamic reactivity and the static and dynamic acidity of α- and γ-$LiAlO_2$, with a special interpretative emphasis on the Li ion. The reason for Li being solely extractable in α-$LiAlO_2$ is found to arise from (i) a difference in Li electrophilicity between α- and γ-phase (frontier band argument), (ii) a significantly smaller energy for Li binding to its neighboring atoms in α- compared to γ-phase (thermodynamic argument), and (iii) a dramatic difference in energetic behavior upon dislocating a Li atom from its equilibrium position in α- and γ-phase (kinetic argument). Additionally, we show how the movement of a local atomic carrier of reactivity and acidity within a nonequilibrium structure can be easily observed by use of computation.

1. Introduction

$LiAlO_2$ was first synthesized by Weyberg in 1906.[1] Up to now, at least five different phases have been described. Especially during this last decade, the fundamental compound has found attention mainly in two very different fields: nuclear physics and solid-state chemistry.

On the one hand, nuclear physicists were interested in the γ-modification of $LiAlO_2$. Because of its good performance under high neutron and electron radiation,[2,3] the phase appears to be a promising lithium ceramic[4,5] suitable as an in situ tritium-breeding material in future fusion reactors.

On the other hand, solid-state chemists investigating preparational routes to $LiAlO_2$ discovered its interesting acid–base chemistry.[6] As Poeppelmeier and Kipp have demonstrated, the α-modification (but *not* the β- or γ-modification) reacts with molten benzoic acid, leading to a nearly total Li^+–proton exchange,[7] thus forming $Li_{1-x}H_xAlO_2$ ($x \geq 0.95$), which probably possesses a cubic spinel structure. Details on the microscopic Li^+–H^+ exchange process are unknown.

We are interested in the astonishing difference in chemical reactivity among the three modifications of $LiAlO_2$. The reason for α being highly reactive and β or γ being totally unreactive is clearly mysterious. As a possible explanation, Rouxel proposed different acid–base qualities for the α-modification (all cations reside in octahedral O environments, having *long* metal–oxygen distances) compared to the β- or γ-modification (all cations are kept in O tetrahedra, with *short* distances).[8]

We will follow this idea and try to *theoretically* describe and explain the experiment performed by Poeppelmeier with the truly chemical language of acid–base interactions. To extend this point of view, reconsider the classic Hargreaves process of synthesizing hydrochloric acid

$$2NaCl + H_2SO_4 = 2HCl + Na_2SO_4$$

where the *weaker* acid HCl is formed ("driven out") by the reaction of a *stronger* acid H_2SO_4 with a salt.[9] Applying this picture to the $LiAlO_2$–benzoic acid reaction, one may assume a competitive process between the Lewis acid Li^+ and the Brønsted acid H^+. *Thus, the difference in reactivity of the different $LiAlO_2$-modifications should be explainable by a difference in their Li cation acidities.*

This approach closely resembles an initial-state model where the main focus is on the roles of the educts. Could one also try to consider a final-state model, looking at the properties of the product phases? Logically, this is *not* possible here since there is only *one* product ($Li_{1-x}H_xAlO_2$), not very well characterized,

[†] On leave from the Max-Planck-Institut für Festkörperforschung, Heisenbergstr. 1, 7000 Stuttgart 80, Germany. Address correspondence to the author at this address.

(1) Weyberg, Z. *Zbl. Mineralog.* **1906**, 645.
(2) Auvray-Gély, M. H.; Dunlop, A.; Hobbs, L. W. *J. Nucl. Mater.* **1985**, *133/134*, 230.
(3) Botter, F.; Lefevre, F.; Rasneur, B.; Trotabas, M.; Roth, E. *J. Nucl. Mater.* **1986**, *141/143*, 364.
(4) Arons, R. M.; Poeppel, R. B.; Tetenbaum, M.; Johnson, C. E. *J. Nucl. Mater.* **1981**, *103/104*, 573.
(5) Schulz, B.; Wedemeyer, H. *J. Nucl. Mater.* **1986**, *139*, 35.
(6) Poeppelmeier, K. R.; Hwu, S.-J. *Inorg. Chem.* **1987**, *26*, 3297.
(7) Poeppelmeier, K. R.; Kipp, D. O. *Inorg. Chem.* **1988**, *27*, 766.
(8) Rouxel, J. Paper presented at the 201st National Meeting of the American Chemical Society, Atlanta, GA, April 1991.
(9) Essentially, the principle of LeChâtelier forces the reaction to the right side since gaseous HCl is driven out.

0020-1669/93/1332-0001$04.00/0

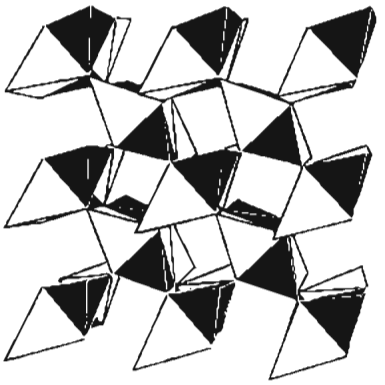

Figure 1. Perspective view of tetragonal γ-$LiAlO_2$, slightly tilted against the 4-fold screw axis. LiO_4 and AlO_4 units are represented with shaded and black tetrahedra, respectively.

Table I. Lattice and Positional Parameters (Standard Deviations) of $LiAlO_2$ Phases

modification	a (pm)	b (pm)	c (pm)	space group (No.)	ref
α	280.03 (6)		1421.6 (3)	$R\bar{3}m$ (166)	22
β	528	630	490	$Pna2_1$ (33)	26
γ	517.15 (3)		628.40 (6)	$P4_12_12$ (92)	19

modification	atom	Wyckoff position	x	y	z	ref
α	Li	3a	0	0	0	22
	Al	3b	0	0	$^1/_2$	
	O	6c	0	0	0.2375	
(β)	Li	4a	0.4207 (14)	0.1267 (11)	0.4936 (97)	27
	(Ga!)	4a	0.0821 (1)	0.1263 (1)	0	
	O(1)	4a	0.4066 (7)	0.1388 (5)	0.8927 (10)	
	O(2)	4a	0.0697 (7)	0.1121 (5)	0.3708 (10)	
γ	Li	4a	0.8126 (9)	x	0	18
	Al	4a	0.1759 (2)	x	0	
	O	8b	0.3369 (4)	0.2906 (4)	0.7723 (4)	

which could only be compared with *itself*. In other words, since all educts are *identical* in chemical composition, we would always get the same product if there would not be differences in reactivity between the different phases of $LiAlO_2$, *completely controlled* by their difference in crystal chemistry.

In this paper, we are going to investigate by means of electronic structure calculations two of those $LiAlO_2$ modifications. After critically examining the structural data, we numerically evaluate the binding and both the static and dynamic reactivity and the static and dynamic acidity of α- and γ-$LiAlO_2$, with a special interpretative emphasis on the Li atom. The quantum-mechanical calculations are performed within the framework of the semiempirical extended Hückel (EH) method[10,11] in its tight-binding approach[12] whereas qualities of reactivity and acidity, i.e. absolute hardness and atomic increments of reactivity and electrophilicity, are computed according to the newly defined theoretical acid–base notion for solids.[13]

2. Structural Information

Our knowledge of the structures of $LiAlO_2$ is still far from complete. The first diffraction studies are due to Hummel[14] and Théry et al.,[15] who observed what is known today as the *tetragonal* γ-modification. It is typically prepared by a high-temperature synthesis (≥1000 °C) from lithium carbonate and aluminum oxide. Using fluxes, high-quality single crystals can be grown easily.[16] The crystal structure of piezoelectric γ-$LiAlO_2$ was solved independently by Bertaut et al.[17] (powder) and by Marezio[18] (single crystal). Probably the most accurate lattice constants are due to Wong-Ng et al.[19] Structural parameters are compiled in Table I, whereas a perspective view is given in Figure 1. γ-$LiAlO_2$ consists of an infinite three-dimensional array of distorted LiO_4 and AlO_4 tetrahedra. Each tetrahedron shares one of its edges with another tetrahedron of different kind, and each vertex of every tetrahedron is shared with two additional tetrahedra, one of each kind.

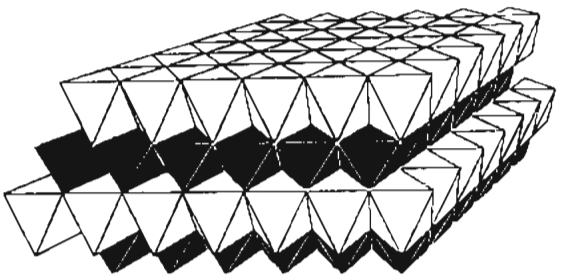

Figure 2. Perspective view of trigonal α-$LiAlO_2$. LiO_6 and AlO_6 units are represented with shaded and black octahedra, respectively.

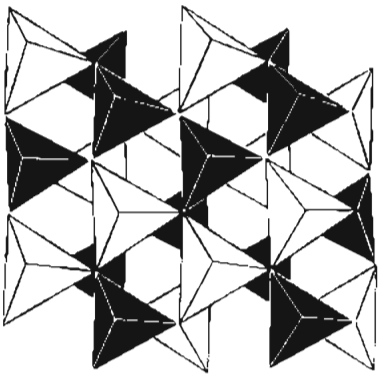

Figure 3. Perspective view of orthorhombic β-$LiAlO_2$, slightly tilted against the 2-fold screw axis. LiO_4 and AlO_4 units are represented with shaded and black tetrahedra, respectively.

The second modification, *trigonal* α-$LiAlO_2$, was first synthesized by Lehmann and Hesselbarth[20] as well as by Lejus and Collongues[21] by a low-temperature procedure (600 °C). It can also be made from the γ-modification by applying both high pressure (35 kbar) and higher temperature (850 °C) as done preceding the structural determination of Marezio and Remeika.[22] The α-phase (Table I) is isostructural with $NaHF_2$ and approximately 30% denser than the γ-phase. As can be seen from Figure 2, α-$LiAlO_2$ is built up from alternating layers of condensed LiO_6 and AlO_6 octahedra.

Orthorhombic β-$LiAlO_2$, the third modification, was first mentioned by Théry[15] as a low-temperature variant, stable below 0 °C.[23] We only know the approximate lattice constants[26] as

(10) Hoffmann, R.; Lipscomb, W. N. *J. Chem. Phys.* **1962**, *36*, 2179.
(11) Hoffmann, R. *J. Chem. Phys.* **1963**, *39*, 1397.
(12) Hoffmann, R. *Angew. Chem.* **1987**, *99*, 871; *Angew. Chem., Int. Ed. Engl.* **1987**, *26*, 846.
(13) Dronskowski, R. *J. Am. Chem. Soc.* **1992**, *114*, 7230.
(14) Hummel, F. A. *J. Am. Ceram. Soc.* **1951**, *34*, 235.
(15) Théry, J.; Lejus, A.-M.; Briançon, D.; Collongues, R. *Bull. Soc. Chim. Fr.* **1961**, 973.
(16) Schwarzer, H.; Neels, H. *Krist. Tech.* **1971**, *6*, 639.
(17) Bertaut, F.; Delapalme, A.; Bassi, G.; Durif-Varambon, A.; Coubert, J. C. *Bull. Soc. Fr. Mineral. Cristallogr.* **1965**, *88*, 103.
(18) Marezio, M. *Acta Crystallogr.* **1965**, *19*, 396.
(19) Wong-Ng, W.; McMurdie, H.; Paretzkin, B.; Hubbard, C.; Dragoo, A. *Powd. Diffract. J.* **1987**, *2*, 111. No. 38–1464, Joint Committee on Powder Diffraction Standards, Swarthmore, PA.
(20) Lehmann, H.-A.; Hesselbarth, H. *Z. Anorg. Allg. Chem.* **1961**, *313*, 117.
(21) Lejus, A.-M.; Collongues, R. *C. R. Hebd. Seances Acad. Sci.* **1962**, *254*, 2005.
(22) Marezio, M.; Remeika, J. P. *J. Chem. Phys.* **1966**, *44*, 3143.
(23) It should *not* be confused with the so-called lithium "β-alumina" phase Li_2O-nAl_2O_3 ($n \approx 5$–11), having a complex spinel block structure[24] in which Li ions are highly mobile.[25]
(24) Peters, C. R.; Bettman, M.; Moore, J. W.; Glick, M. D. *Acta Crystallogr.* **1971**, *B27*, 1826.

well as the refined structural parameters (Table I) of the isotypic Ga phase β-$LiGaO_2$ from the work of Marezio.[27] The crystal structure (Figure 3) can be described as a three-dimensional network of LiO_4 and AlO_4 tetrahedra having only vertices in common. Each atom is tetrahedrally coordinated.

A *monoclinic* high-pressure modification (confusingly called "β-$LiAlO_2$") was announced by Chang and Margrave.[28] On the basis of infrared data, they speculated that this phase might contain both tetrahedra and octahedra, although an explicit crystal structure determination was not attempted.

The systematic absences in their powder diffraction data correspond to space groups *P*2, *Pm*, and *P*2/*m*. The reported monoclinic lattice constants give rise to unit cell volumes which equal 9.69, 9.99, and 12.65 times the molar volumes of α-, β-, and γ-$LiAlO_2$. This seems very unusual for a monoclinic structure, especially if the multiplicities of general and special positions are taken into account. In addition, the marginal difference (0.05%) between the *b* axis of orthorhombic β-$LiAlO_2$ and the monoclinic *c* axis as well as the nearly *integer* relation in molar volumes (9.99) between these phases, likewise in conflict with the assumption of both 4- *and* 6-fold coordination, causes us some dissatisfaction with the proposed monoclinic cell. However, we were unable, using the DELOS program,[29] to reduce the monoclinic cell by a Delaunay procedure[30] to a cell of the preceding modifications, thus implying a group–subgroup relationship.

Finally, a *cubic* form, synthesized[31] by reducing corundum with lithium hydride at about 500 °C, was characterized by Debray and Hardy.[32] The unit cell (a = 1265.0 (5) pm, space group $I4_132$) contains 48 formula units, and the molar volume is practically identical with the one of γ-$LiAlO_2$, suggesting 4-fold coordination for both Li and Al atoms.

In order to estimate the qualities of atomic structural parameters for α-, β-, and γ-$LiAlO_2$, we recalculated[33] the nearest metal atom–O atom distances as well as the empirical *valences* (Table II) according to the bond length–bond strength formula of Brown and Altermatt.[34] The bond strength s is given by the expression

$$s = \exp\left(\frac{r_0 - r}{37\ \text{pm}}\right) \qquad (1)$$

and the atomic valence v is identical to the sum of the bond strengths:

$$v = \sum_i s_i \qquad (2)$$

The highly accurate (fitted to 333 and 397 crystal structures) single-bond distances r_0 are 146.6 (3) and 165.1 (2) pm for Li–O and Al–O combinations, respectively. From Table II it is obvious that only in α- and γ-$LiAlO_2$ do the valences of Li and Al equal approximately the expected values of 1 and 3, respectively. The valence of Al in the β-phase is too small since the refined parameters of the isotypical Ga phase were used, giving too large Al–O distances.

With respect to the structural data, more information is needed on the reported cubic and especially on the monoclinic modification. An independent refinement would be desirable for the β-phase since we cannot computationally optimize its structural parameters. Thus, only the trigonal α- and the tetragonal γ-modification will be investigated in the following.

Table II. Nearest Li–O and Al–O Distances (pm) and Empirical Valences in $LiAlO_2$ Phases[a]

modification	d_{Li-O} (pm)	v_{Li}	d_{Al-O} (pm)	v_{Al}	v_O
α	211.4 (6×)	1.04	190.5 (6×)	3.02	−2.03
(β)	192.1	1.08	179.4	2.58	−1.84
	195.1		181.6		
	195.8		182.0		
	196.8		182.3		
γ	195.2 (2×)	0.94	175.9 (2×)	2.96	−1.95
	206.1 (2×)		176.7 (2×)		

[a] The standard deviations of the interatomic distances lie below 2 pm for the α- and below 5 pm for the γ-modification. For the β-modification the errors are huge (see discussion). The valence value for the O atom in β-$LiAlO_2$ is the average of the practically equivalent O(1) and O(2) atoms.

3. Physical Data

Lehmann and Hesselbarth report[20] that the conversion of the high-pressure α-modification into the γ-phase is initiated at 650 °C whereas Lejus states 900 °C.[35] During the transformation, the heating curve shows *no* appreciable thermal effect.[20] However, it seems reasonable for us to regard the γ-modification as the thermodynamic stable phase since the α–γ transformation is *irreversible* and the γ-phase is maintained even upon slow cooling.[20]

In fair agreement with earlier communications[36,37] the melting point of γ-$LiAlO_2$ was given[38] as 1923 K although Lejus claims that γ-$LiAlO_2$ already converts to $LiAl_5O_8$ at 1300 °C.[35] Using measurements of heats of solution, Coughlin obtained the following value for the formation enthalpy[39] of γ-$LiAlO_2$ at room temperature

$$\Delta H^0_{f,298.15}(\gamma) = -1189.6\ (9)\ \text{kJ/mol}$$

whereas the corresponding value for absolute zero, corrected by the integrated low-temperature heat capacity,[40] lies at

$$\Delta H^0_{f,0}(\gamma) = -1183.2\ \text{kJ/mol}$$

Besides the recent nuclear investigations (section 1), no physical measurements on γ-$LiAlO_2$ were published other than those of infrared[41-43] and Raman[44] spectroscopy.

4. Electronic Structure

Two ab initio calculations on the high-temperature *molecule* $LiAlO_2$ have already been performed.[45,46] They favor a linear $C_{\infty v}$ geometry Li–O–Al–O with respect to a C_{2v} molecular ring by approximately 53 kJ/mol. Our calculations are the first ones for the extended solid.

For the geometry of α-$LiAlO_2$, the hexagonal setting of the trigonal structure was used. The unit cell then contained three

(25) Whittingham, M. S.; Huggins, R. A. *J. Chem. Phys.* **1971**, *54*, 414.
(26) No. 33-785, Joint Committee on Powder Diffraction Standards, Swarthmore, PA (private communication from General Electric Co., Schenectady, NY, 1978).
(27) Marezio, M. *Acta Crystallogr.* **1965**, *18*, 481.
(28) Chang, C. H.; Margrave, J. L. *J. Am. Chem. Soc.* **1968**, *90*, 2020.
(29) Burzlaff, H.; Zimmermann, H. *Z. Kristallogr.* **1985**, *170*, 241, 247.
(30) Delaunay, B. *Z. Kristallogr.* **1933**, *84*, 109.
(31) Hagenmüller, P.; Debray, L. *C. R. Hebd. Seances Acad. Sci.* **1960**, *250*, 3847.
(32) Debray, L.; Hardy, A. *C. R. Hebd. Seances Acad. Sci.* **1960**, *251*, 725.
(33) Busing, W. R.; Masten, K. D.; Levy, J. A. Program ORFFE-3. Report ORNL-TM-306, Oak Ridge National Laboratory: Oak Ridge, TN, 1971.
(34) Brown, I. D.; Altermatt, D. *Acta Crystallogr.* **1985**, *B41*, 244.
(35) Lejus, A.-M. *Rev. Hautes Temp. Refract.* **1964**, *1*, 53.
(36) Ballő, R.; Dittler, E. *Z. Anorg. Allg. Chem.* **1912**, *76*, 39.
(37) Kim, K. H.; Hummel, F. A. *J. Am. Ceram. Soc.* **1960**, *43*, 611.
(38) Ikeda, Y.; Ito, H.; Matsumoto, G. *J. Nucl. Mater.* **1981**, *97*, 47.
(39) Coughlin, J. P. *J. Am. Chem. Soc.* **1957**, *79*, 2397.
(40) King, E. G. *J. Am. Chem. Soc.* **1955**, *77*, 3189.
(41) Murthy, M. K.; Kirby, E. M. *J. Am. Ceram. Soc.* **1962**, *45*, 324.
(42) Schroeder, R. A.; Lyons, L. L. *J. Inorg. Nucl. Chem.* **1966**, *28*, 1155.
(43) Tarte, P. *Spectrochim. Acta* **1967**, *A23*, 2127.
(44) Ignat'ev, I. S.; Lazarev, A. N.; Kolesova, V. A. *Izv. Akad Nauk SSSR, Neorg. Mater.* **1976**, *12*, 1230; *Inorg. Mater. (Engl. Transl.)* **1976**, *12*, 1024.
(45) Musaev, D. G.; Yakobson, V. V.; Charkin, O. P. *Zh. Neorg. Khim.* **1989**, *34*, 1946; *Russ. J. Inorg. Chem.* **1989**, *34*, 1106.
(46) Bencivenni, L.; Pelino, M.; Ramondo, F. *THEOCHEM* **1992**, *253*, 109.
(47) Ramirez, R.; Böhm, M. C. *Int. J. Quantum Chem.* **1988**, *34*, 571.

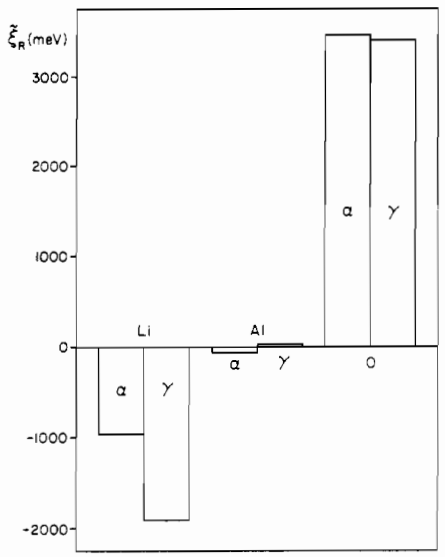

Figure 4. Simplified atomic *reactivity* increments $\tilde{\xi}_R$ (meV) for α- and γ-$LiAlO_2$.

formula units (12 atoms). The irreducible wedge of the Brillouin zone was equally spaced[47] by 48 *k*-points. For γ-$LiAlO_2$, the tetragonal cell with four formula units and 16 atoms was taken. The number of *k*-points was 45.

4.1. Static Calculations. The EH theory's exchange integrals for Li, Al, and O were taken from the literature.[11,48,49] The orbital exponents were refined as described in Appendix A.

The total valence energies are

$$E^0(\alpha) = -315.13 \text{ eV} \qquad E^0(\gamma) = -316.80 \text{ eV}$$

supporting the assumption of γ-$LiAlO_2$ being *more* stable than α-$LiAlO_2$. However, a comparison of the experimental formation enthalpy of Coughlin (section 3) with the ones that can be calculated from our theoretical total energies shows the latter energies to be too large. The cohesive energy (total binding energy) is given by the difference of the total energy E^0 and the atomic energies (H_{ii} values) of the constituent atoms. Extrapolating this absolute zero temperature value by the experimental heat capacity (6.4 kJ/mol if integrated up to 298.15 K; see section 3) and subtracting the atomic sublimation enthalpies $\Delta H^0_{s,298.15}$,[50] we arrive at the following theoretical formation enthalpies

$$\Delta H^{EH}_{f,298.15}(\alpha) = -1668.5 \text{ kJ/mol} \qquad \Delta H^{EH}_{f,298.15}(\gamma) = -1830.0 \text{ kJ/mol}$$

largely overestimating the experimental result. This is a poor result for the theoretical total energies. However, the *difference* in total energies between both phases (about 162 kJ/mol), calculated by only taking covalency into account, is large enough to be significant. On the other hand, a conceptionally very different calculational route, namely computing the difference in electrostatic Madelung energies[51] of the α- and γ-phases also leads to an astonishingly large enthalpy difference (roughly 117 kJ/mol). Thus, it is shown that the significantly higher stability of γ is not a computational artifact. Therefore, the enthalpy difference should be detectable by an accurate thermoanalytic measurement.

The *absolute hardness* energies[52] η were computed according

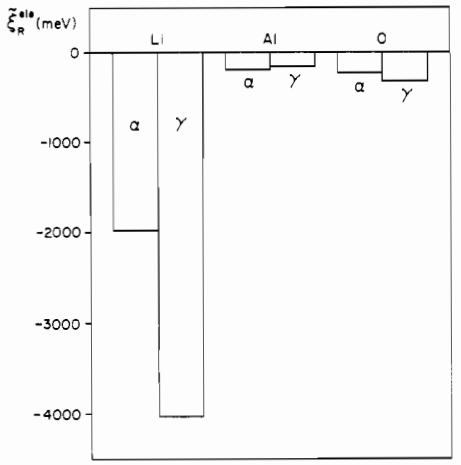

Figure 5. Simplified atomic *electrophilicity* increments $\tilde{\xi}^{ele}_R$ (meV) for α- and γ-$LiAlO_2$.

to the three-point finite-difference approximation

$$\eta \approx \frac{1}{2}(E^+ + E^-) - E^0 \equiv \sum_R \xi_R \tag{3}$$

which was recently shown to be partitionable into atomic increments of reactivity ξ_R (see below).[13] E^+, E^-, and E^0 stand for the total energies of the single positively charged, single negatively charged, and the neutral system. The absolute hardness η is the second derivative of *E* with respect to *N* (electron number) which appears in density-functional theory.[53] It serves as a *resistance indicator* of molecules[53] and solids[13] against electronic (chemical) attack. Inert systems have a high η whereas reactive systems have a small η. The absolute hardness can also be divided[13] into *electrophilic* and *nucleophilic energy changes* $\Delta E^{ele(nuc)}$ which themselves are composed of atomic *increments* of *electrophilicity and nucleophilicity* $\xi^{ele(nuc)}_R$:

$$\Delta E^{ele(nuc)} \approx E^{-(+)} - E^0 \equiv \sum_R \xi^{ele(nuc)}_R \tag{4}$$

For the absolute hardnesses of $LiAlO_2$ modifications, we arrive at

$$\eta(\alpha) = 5.89 \text{ eV} \qquad \eta(\gamma) = 4.92 \text{ eV}$$

stating that the high-pressure modification, having the higher η value, is *less* sensitive to electronic perturbations. The acidic contributions to η, the electrophilic energy changes, are

$$\Delta E^{ele}(\alpha) = -2.63 \text{ eV} \qquad \Delta E^{ele}(\gamma) = -4.85 \text{ eV}$$

This means that the tetragonal γ-modification, *inert* if exposed to molten benzoic acid, has a *stronger* electrophilic tendency since its energy gain while accepting additional charge would be higher than that of α-$LiAlO_2$. In chemical language, benzoic acid exchanges its proton with a Li ion only if in contact with the *weaker* $LiAlO_2$ acid.

The atoms' roles concerning reactivity and acidity are locally detected by atomic increments of reactivity ξ_R and electrophilicity ξ^{ele}_R. *Simplified* increments (assuming (i) all exchange integrals to be energy-independent and (ii) all core bands to be frozen) can be formulated[13] as

$$\tilde{\xi}_R = \frac{1}{2}\sum_{\mu \in R}^{\mu}\left\{h_{\mu\mu}\left(\int_{\mathcal{E}_F^0}^{\mathcal{E}_F} P_{\mu\mu}(\mathcal{E})\,d\mathcal{E} - \int_{\mathcal{E}_F^+}^{\mathcal{E}_F^0} P_{\mu\mu}(\mathcal{E})\,d\mathcal{E}\right) + \sum_{R'}\sum_{\nu \in R'}^{\nu} h_{\mu\nu}\left(\int_{\mathcal{E}_F^0}^{\mathcal{E}_F} \mathcal{R}[P_{\mu\nu}(\mathcal{E})]\,d\mathcal{E} - \int_{\mathcal{E}_F^+}^{\mathcal{E}_F^0} \mathcal{R}[P_{\mu\nu}(\mathcal{E})]\,d\mathcal{E}\right)\right\} \tag{5}$$

(48) Garfunkel, E. L.; Minot, C. *J. Solid State Chem.* **1986**, *65*, 72.
(49) Anderson, A. B.; Hoffmann, R. *J. Chem. Phys.* **1974**, *60*, 4271.
(50) Emsley, J. *The Elements*; Clarendon Press: Oxford, U.K., 1991.
(51) Hoppe, R. *Angew. Chem.* **1966**, *78*, 52; **1970**, *82*, 7.
(52) Parr, R. G.; Pearson, R. G. *J. Am. Chem. Soc.* **1983**, *105*, 7512.
(53) Parr, R. G.; Yang, W. *Density-functional theory of atoms and molecules*; Oxford University Press: New York, 1989.

and

$$\tilde{\xi}_R^{ele} = \sum_{\mu \overset{\mu}{\in} R} \left\{ h_{\mu\mu} \int_{\mathcal{E}_F^0}^{\mathcal{E}_F} P_{\mu\mu}(\mathcal{E})\, d\mathcal{E} + \sum_{R'} \sum_{\nu \overset{\nu}{\in} R'} h_{\mu\nu} \int_{\mathcal{E}_F^0}^{\mathcal{E}_F} \mathcal{R}[P_{\mu\nu}(\mathcal{E})]\, d\mathcal{E} \right\} \quad (6)$$

h and P symbolize the one-electron Hamiltonian and the one-electron density matrix, and the real parts of the complex off-diagonal entries are characterized by $\mathcal{R}$. The $\mathcal{E}_F$'s are the varying Fermi energies up to which the integrations have to be carried out.

As a general rule, the lower the increments (which are energy values) the higher the reactivity and acidity.[54] A highly reactive (acidic) atom has a larger associated *negative* increment of reactivity (electrophilicity). On the contrary, an atom showing no sign of reactivity (acidity) is characterized by a large *positive* increment of reactivity (electrophilicity).

Simplified atomic reactivity and electrophilicity increments can be found in Figures 4 and 5, respectively. In harmony with chemical intuition, Li atoms turn out to be the most reactive, Al atoms are intermediately reactive, and O atoms are inert. Because of their deep-lying bonding levels with mainly O character, O atoms are indeed very insensitive to what is going on at the Fermi energy $\mathcal{E}_F$ (frontier bands). In contrast to this, Li atoms form the reactive parts in both modifications since their associated energy levels are very close to $\mathcal{E}_F$. In short, an inert Al–O network contains reactive (and possibly mobile; see section 4.2) Li atoms.

Moreover, the Li atoms' electrophilicities (Figure 5) run parallel with their reactivities, and they are larger than those of Al and O. So the $\tilde{\xi}_R^{ele}$ values tell us that high-lying Li-centered bands will be mostly stabilized in energy if excess electrons can be inserted. However, as could already be inferred from the electrophilic energy changes, it is the *less* acidic Li atom (in α-$LiAlO_2$) which is exchanged in the reaction of Poeppelmeier! In acid–base language, the Li atom in γ-$LiAlO_2$ is a too strong Lewis acid for the benzoic acid's proton to "drive out".

At this point the calculation might seem to be in conflict with the intuition of a chemist who might expect that the *more* acidic Li atom is exchanged against a proton. Indeed, intuition would probably favor Li in 6-coordination (α) to be more acidic, since it has a slightly higher charge, visible from the list of empirical valences in Table II. However, acidic behavior is characterized not by atomic charge but by the tendency to fill hitherto unfilled levels or bands, i.e. to attract electron density. In this respect, Li in α is *less* acidic. Moreover, this finding is the only possibility which coincides with considerations on energies of binding to the Al–O matrix and on calculations simulating kinetics (see below).

This argumentation would imply that an even *weaker* Lewis acid than Li in α-$LiAlO_2$ could always be exchanged by an incoming proton. Ignoring all chemical experience, one would then be tempted to assume that even Al^{3+} ions could be good candidates for replacement by H^+ although simple electrostatics reasoning should rule out such an event. Moreover then, another serious condition would not be fulfilled. Of course, there is also the question whether the release of a bonded cation is energetically favorable or not! The contribution of a single atom R for the total valence energy of a three-dimensional crystal can generally be formulated as

$$E_R = \int d\vec{k} \int^{\mathcal{E}_F} d\mathcal{E} \left\{ \underbrace{\sum_{\mu \overset{\mu}{\in} R} h_{\mu\mu} P_{\mu\mu}(\mathcal{E},\vec{k})}_{\text{on-site term}} + \underbrace{\sum_{\mu \overset{\mu}{\in} R} \sum_{R'} \sum_{\nu \overset{\nu}{\in} R'} \mathcal{R}[h_{\mu\nu} P_{\mu\nu}(\mathcal{E},\vec{k})]}_{\text{off-site term}} \right\} \quad (7)$$

where the first (*net*) part of this *gross* atomic energy is located on the atom's site (therefore called the "on-site" term) and the second part arises from the interaction of atom R with *all* its surrounding neighbors ("off-site" term).

For Li and Al, these off-site terms over all bonding and antibonding interactions (which we will call E^{off} from now on) are mainly dominated by the strong bonding interaction with the nearest coordination shell of O atoms, but they also include the smaller antibonding contributions from second-nearest metal atom neighbors, plus all even smaller influences beyond this shell. We find the off-site energies to be

$$E_{Li}^{off}(\alpha) = -18.30 \text{ eV} \qquad E_{Li}^{off}(\gamma) = -24.25 \text{ eV}$$
$$E_{Al}^{off}(\alpha) = -36.99 \text{ eV} \qquad E_{Al}^{off}(\gamma) = -38.53 \text{ eV}$$

leading us to the following conclusions:

First, Li atoms are more weakly bonded within the structural matrix than Al atoms. So while theoretically extracting a metal (M) atom from α- or γ-$LiAlO_2$, the remaining lattice is *less* destabilized if M = Li than if M = Al. From a thermodynamic point of view, this result strongly favors the release of Li compared to Al!

Second, there is a big difference in Li binding energy between α- and γ-phase, but only a small one for Al. Let us assume the chemical bonding of Li to result mainly from its singly filled 2s level. A simple molecular calculation on LiO_4^{7-} and LiO_6^{11-} indeed reveals the overlap integral S_{ij} of Li-2s–O-2s in the totally symmetric a_1 bonding combination of the tetrahedron ($d_{Li-O} \approx$ 201 pm) to be roughly 10% *larger* than the corresponding S_{ij} in the a_{1g} combination of the octahedron ($d_{Li-O} \approx$ 211 pm). But also the small S_{ij} of Li-2p–O-2p of the tetrahedral t_2 combination is *less negative* than the S_{ij} of the octahedral t_{1u}. As a result, the total overlap population (and the off-site energy) around Li is larger in γ-$LiAlO_2$ than in α-$LiAlO_2$. Thus, indeed the less acidic Li atom within α (which is exchanged in Poeppelmeier's reaction) is *thermodynamically* more easily released.

But why are the off-site energies of Al so similar, although the differences in the bond distances between AlO_4 tetrahedron ($d_{Al-O} \approx$ 176 pm) and AlO_6 octahedron ($d_{Al-O} \approx$ 191 pm) are even larger? A similar model calculation on AlO_4^{5-} and AlO_6^{9-} shows the overlap integral S_{ij} of Al-3s–O-2s to be about 11% *smaller* than the corresponding integral in the octahedron. However, there is the singly *occupied* 3p level centered on Al, engaged in the t_2 (t_{1u}) bonding combination of tetrahedron (octahedron), and here the S_{ij} of Al-3p–O-2p is about 4 times larger in AlO_4^{5-}, finally leading to similar overlap population values for both polyhedra. Thus, the approximate constancy of the off-site energy for Al in both modifications is the result of a delicate a_1/t_2 and a_{1g}/t_{2u} balance.

At the end of this section we wish to emphasize that the important energetic difference between the bonding of Li atoms in α- and γ-$LiAlO_2$ is an essential quantum-mechanical result. It is not reflected by the empirical valences in Table II which claim the Li atoms to be practically identical in both phases. *In this respect, the simplest (ionic) model fails within an ionic crystal.* Thus, the bond length–bond strength concept, although highly useful in the assessment of structural data, should not be extended to give conclusions about energetics.

(54) Dronskowski, R.; Hoffmann, R. *Adv. Mater.* **1992**, *4*, 514.

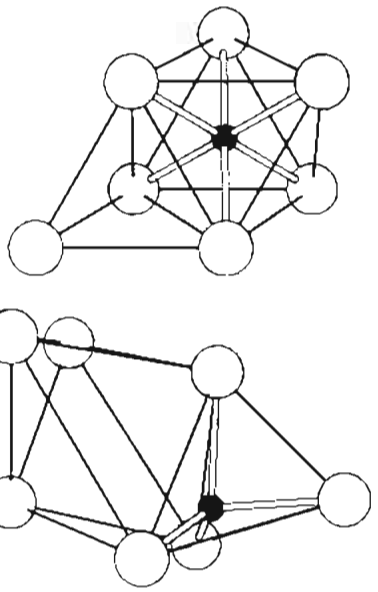

Figure 6. Top: LiO_6 octahedron and neighboring tetrahedral hole within α-$LiAlO_2$. Bottom: LiO_4 tetrahedron and neighboring octahedral hole within γ-$LiAlO_2$.

4.2. Dynamic Calculations. So far, our arguments are based on frontier orbital concepts (reactivity and electrophilicity increments) as well as on thermodynamic ideas (off-site energies). One can, however, go another step forward and try to investigate the *initial act* of exchanging Li^+ with a proton. At the very beginning, a Li ion must escape its coordinating environment of O atoms. We then ask for the geometrical pathway of such a Li ion and its local electronic structure while it is going to move through the remaining structural framework. This is a more *kinetic* point of view.

In Figure 6 we show the local environment of Li within α- and γ-$LiAlO_2$. The perspective view of the LiO_6 octahedron in the α-phase coincides with the hexagonal c axis, and it corresponds to a view which falls exactly onto the layers of octahedra shown in Figure 2. A Li atom in α-$LiAlO_2$ has three neighboring tetrahedral holes, made from the edge-sharing LiO_6 octahedra. We show one of these holes, sharing its triangular face with the LiO_6 octahedron.

The perspective view onto the LiO_4 tetrahedron of γ-$LiAlO_2$ is identical to the one used in Figure 1. Actually, it is the central shaded tetrahedron of Figure 1 which is shown in the ball-and-stick representation. In γ-$LiAlO_2$, all LiO_4 tetrahedra have two neighboring empty O octahedra. Each one shares one of its triangular faces with the LiO_4 tetrahedron. From this polyhedral perspective, α- and γ-$LiAlO_2$ have *complementary* structures.

A migrating Li ion could only enter an interstitial neighboring site. In the α-phase there would result a Li-centered tetrahedral hole, attached to a now empty octahedral O vacancy, and in the γ-phase we would have an octahedral hole occupied by Li, attached to a now empty tetrahedral O vacancy. Both cases could be described as classic Frenkel defects, similar to those found in solid AgCl. From now on, we will assume a *direct interstitial mechanism where the Li ion jumps through a triangular window into the neighboring hole.*

The triangular windows are drawn in Figure 7, for both α- and γ-$LiAlO_2$. Because of the comparatively small size of the O window and the expected internuclear Li–O repulsion, a Li ion has to pass through the *center* of the O triangle, where it faces three short O contacts of 176.6 (α) and 193.4 pm (γ).[55] These distances correspond to empirical valences (see section 2) of 1.33 (far too large) and 0.85 (a bit too small) for the α- and

(55) For simplicity, we assume the O triangles to be completely rigid. The activation barriers to be computed thus represent *upper limits* in energy.

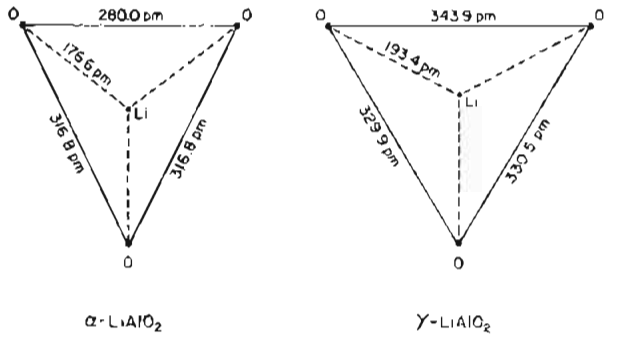

Figure 7. Left: O triangle face of a LiO_6 octahedron within α-$LiAlO_2$. Right: O triangle face of a LiO_4 tetrahedron within γ-$LiAlO_2$. The location of the penetrating Li atom, its distances to the corner O atoms, and the size of the O triangle are indicated (pm).

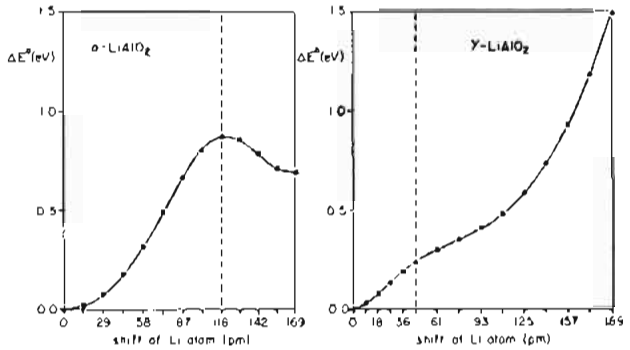

Figure 8. Total energy changes ΔE^0 (eV) within α-$LiAlO_2$ (left) and γ-$LiAlO_2$ (right) as a function of the shift of a moving Li atom (pm). The dashed lines indicate the border between octahedral hole/tetrahedral hole (left) and tetrahedral hole/octahedral hole (right).

γ-modifications, respectively. Thus, the first part of such a Li dislocation may be expected to show a high barrier in α and a smaller one in γ.

Arriving in the tetrahedral vacancy of the α-modification, a Li atom has four Li–O distances of 184 pm, which correspond to a too large empirical valence of 1.45. Additionally, there is one short Li–Li contact of 189 pm. The situation within the γ-phase seems to be more promising for leaving: A Li atom can jump into a slightly off-center position within the octahedral vacancy (at 1/2,0,0, coinciding with the 4-fold screw-axis), having Li–O distances of 173, 206, 224, 243, 250, and 267 pm. Then the empirical valence lies at 0.99, a perfect value. However, there are two further Li–Li contacts of 245 pm and one Li–Al contact of 191 pm whose electronic influence we cannot estimate empirically.

Summarizing the empirical bond length–bond strength criteria for a direct interstitial process, the release of a Li atom is undoubtedly more favorable within γ-$LiAlO_2$ than within α-$LiAlO_2$. Moreover, the Li atom having arrived in the distorted octahedral environment of the γ-phase, a further movement of this atom along the open channel parallel with the c axis (see Figure 1) seems to be easy. *However, this argument contradicts the implications of Poeppelmeier's experiment where α-$LiAlO_2$ exchanges Li^+ easily against a proton, but γ-$LiAlO_2$ does not.*

To solve this paradox, a series of electronic structure calculations was performed. For the proper treatment of core shell repulsion, an additional Li-1s level was included (see Appendix B). Within α-$LiAlO_2$, *one* of the three equivalent Li atoms was pushed toward the center of the neighboring tetrahedral vacancy. The distance $d_I(\alpha)$ to the triangular O window is 116 pm (reached in eight steps of 14.5 pm), followed by the second movement $d_{II}(\alpha)$ of 53 pm (cut into four steps of 13 pm) when the tetrahedral center is reached.

Likewise, *one* of the four symmetry-equivalent Li atoms in γ-$LiAlO_2$ was shifted in a stepwise manner into the neighboring

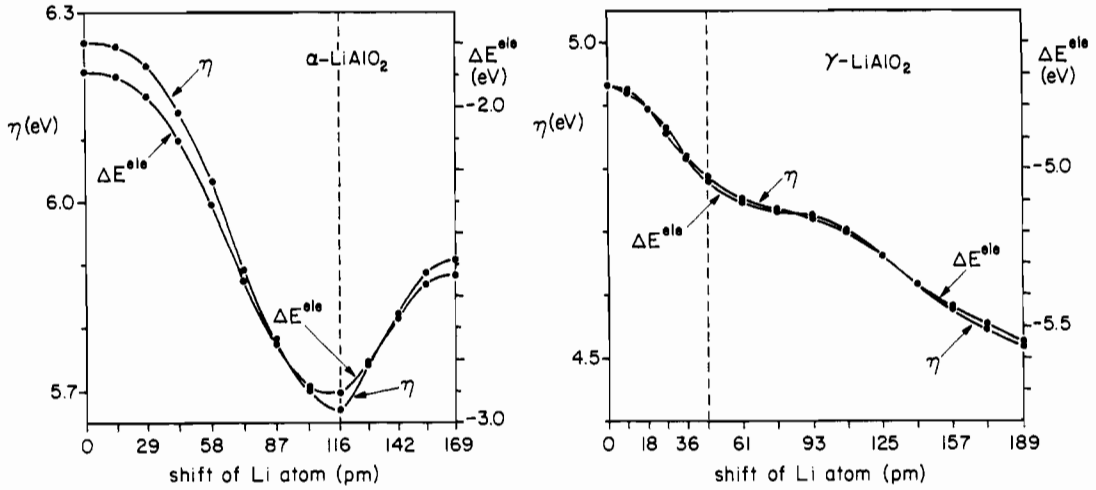

Figure 9. Course of absolute hardness η (eV) and electrophilic energy change ΔE^{ele} (eV) for α-$LiAlO_2$ (left) and γ-$LiAlO_2$ (right) as a function of the shift of the moving Li atom (pm). The dashed lines indicate the border between octahedral hole/tetrahedral hole (left) and tetrahedral hole/octahedral hole (right).

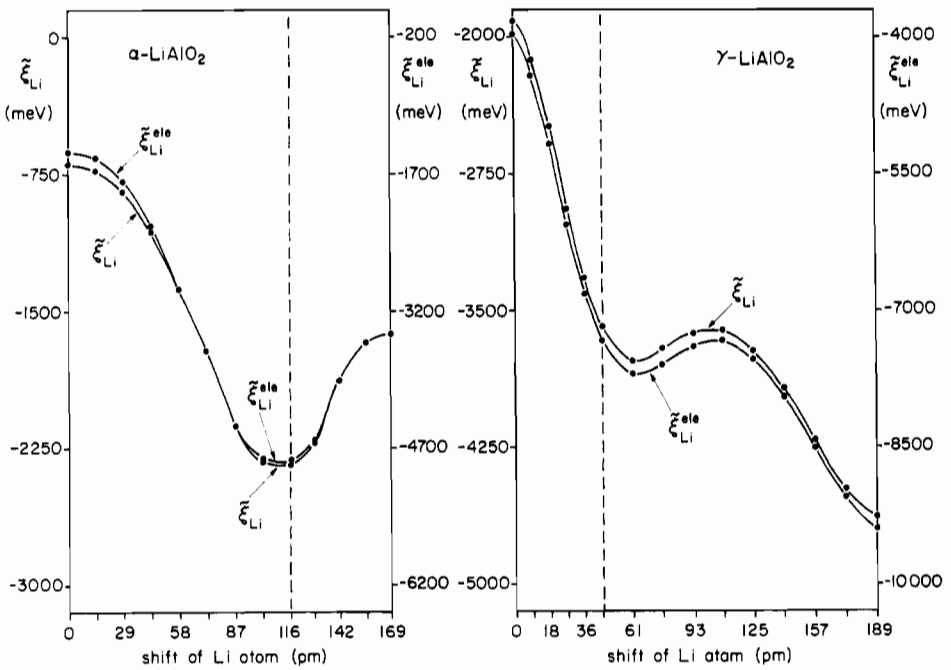

Figure 10. Course of simplified Li *reactivity* increment $\tilde{\xi}_{Li}$ (meV) and simplified Li *electrophilicity* increment $\tilde{\xi}_{Li}^{ele}$ (meV) for α-$LiAlO_2$ (left) and γ-$LiAlO_2$ (right) as a function of the shift of the moving Li atom (pm). The dashed lines indicate the border between octahedral hole/tetrahedral hole (left) and tetrahedral hole/octahedral hole (right).

distorted octahedral environment. The drift distance $d_I(\gamma)$ is 45 pm (five steps of 9 pm) whereas $d_{II}(\gamma)$ is 144 pm (nine steps of 16 pm).

The computational results (Figure 8) are given as total energy changes versus Li atom dislocations. As expected, the shift of a Li atom within the α-phase involves a high activation barrier of approximately 0.87 eV. This is comparable with typical activation barriers for Na^+ migration into extrinsic (thermally induced) vacancies of NaCl (0.65–0.85 eV).[56] The energy top is reached exactly at the border between octahedral and tetrahedral sites. Equally important, however, is the existence of a *relative minimum* (0.69 eV) for tetrahedral coordination. *Thus, there is finite probability for Li to rest within the O tetrahedron.*

The situation for γ-$LiAlO_2$ is totally different. Only about 0.23 eV is needed to release the Li atom from its tetrahedral coordination and promote it to the triangle window, comparable with the activation barrier of Na^+ within "β-alumina" (0.16 eV).[56]

(56) West, A. R. *Solid State Chemistry and its Applications*; Wiley: New York, 1984; Chapter 13.

This finding is in good agreement with the preceding conclusions based on empirical valences. However, the following path leads to more and more *destabilizing effects*, resulting from the competition of both attractive (Li–O) and repulsive (Li–Li, Li–Al) interactions. *Thus, with up to at least 1.49 eV of activation energy provided, the Li atom will always fall back into its tetrahedral origin.* This sharp contrast between the behavior of Li in α- and γ-$LiAlO_2$, which could not be estimated from the simplest (ionic) model, is in good agreement with the suggestions taken from the acid–base chemistry of $LiAlO_2$ with molten benzoic acid.

How does a stepwise dislocation of a Li atom influence the whole crystal's reactivity and acidity? Figure 9 shows the course of both (i) total hardness η and (ii) electrophilic energy change ΔE^{ele} for α- and γ-$LiAlO_2$. Two conclusions can be drawn. First, the crystal's reactivity (which *increases* as η decreases while Li approaches the O triangle) *parallels* the changes in the total energies. So the phases become not only more destabilized but also more *internally reactive*. Second, the changes in η arise

Table III. EH Energy Parameters for $LiAlO_2$[a]

atom	orbital	H_{ii} (eV)	ζ^{α}	ζ^{γ}
Li	2s	−9.00	1.024	1.060
	2p	−8.00	1.018	1.018
Al	3s	−12.30	1.299	1.745
	3p	−6.50	1.488	1.496
O	2s	−32.30	2.160	2.160
	2p	−14.80	2.170	2.170

[a] The $\zeta^{\alpha,\gamma}$'s are the optimized Slater-type orbital exponents used for α- and γ-$LiAlO_2$ (Appendix A), respectively. An additional Li-1s core orbital with $H_{ii} \equiv -63.00$ eV and $\zeta \equiv 2.66$ was introduced for the simulation of the Li atom movement (Appendix B).

almost completely from the changes in ΔE^{ele} which becomes more negative. This is a clear hint that the dislocation of an acidic atom (Li) from its equilibrium position inevitably leads to an *acidification* of the whole crystal. Thus, the electronic structure calculations have recovered the principle of LeChâtelier: Applying a chemical force (attack of benzoic acid) to a chemical system ($LiAlO_2$) results in a change of the system's chemistry (acidification) such that it may better resist the force.

Finally, Figure 10 shows the *local* changes in reactivity and acidity of the moving Li atom, measured by the simplified atomic increments of reactivity and electrophilicity. Again, two statements can be made. First, the center of reactivity of the crystal is clearly located on the moving Li atom since all other increments (not shown here) stay practically at the same numerical value. For Li in the α-phase, the highest reactivity is reached while it passes the O triangle. For the γ-phase, there is a relative reactivity minimum at 61-pm dislocation, increasing again shortly after. Second, the movement of a Li ion is an *acidic process*, recognizable from the parallel behavior of $\tilde{\xi}_{Li}$ and $\tilde{\xi}^{ele}_{Li}$.

To summarize, we have shown the different reactivities of α- and γ-$LiAlO_2$ with molten benzoic acid to result from three different but associated electronic conditions. First, the Li atom is generally the most reactive and acidic atom within the studied phases. However, it is the *less* acidic Li atom (in α-$LiAlO_2$) which is exchanged against a proton. Second, the complete release of a Li atom is energetically much more favorable over the equally imaginable release of an Al atom. Again, the less acidic Li atom (in α-$LiAlO_2$) is most easily extractable since its binding to the structural matrix is *weakest*. Third, despite having a high activation barrier, a Li atom in α-$LiAlO_2$ has a finite chance to escape from its equilibrium position, in contrast to the situation in γ-$LiAlO_2$, where a Li atom would have to climb up an increasingly steeper energy hill. During the direct interstitial process investigated, the crystal's changes in reactivity and acidity can be easily traced back to the single moving Li atom. The last observation confirms an earlier assumption[13] that increments of reactivity and electrophilicity are useful tools to detect *local* electronic events in an electronically completely delocalized system (extended crystal).

Acknowledgment. R.D. thanks Prof. Roald Hoffmann for his continuous and encouraging support as well as the Verband der Chemischen Industrie (Germany) for financing his and his family's life in Ithaca, NY, by means of a Liebig scholarship. Thanks are also directed to Prof. Jean Rouxel for pointing out this interesting problem. It is a pleasure to thank Jane Jorgensen for her expert drawings. Also, the pleasant working atmosphere provided by all members of Prof. Hoffmann's research group is greatly appreciated. The research at Cornell University was supported by the National Science Foundation through Grant CHE-8912070.

Appendix A. Orbital Exponent Refinement

Fixed approximate atomic wave functions such as Slater orbitals

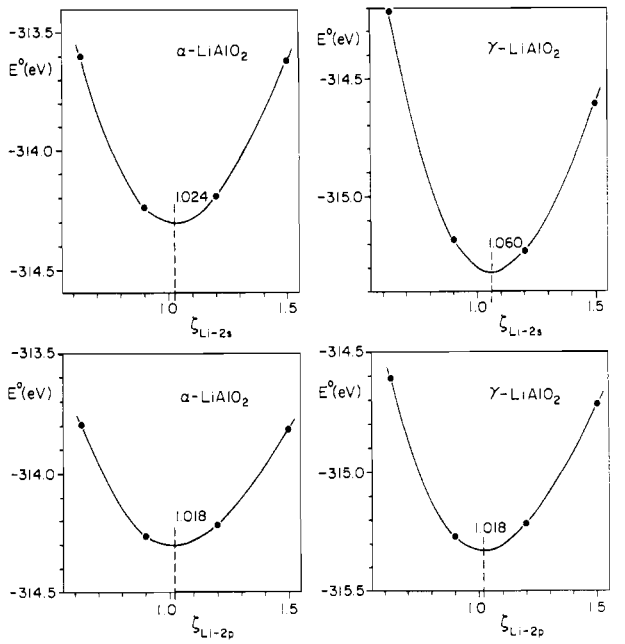

Figure 11. Refinement of the Li-2s (top) and Li-2p (bottom) Slater-type orbital exponents ζ within α-$LiAlO_2$ (left) and γ-$LiAlO_2$ (right). The exponent values leading to the lowest total energies E_0 (eV) are indicated by dashed lines.

$$\phi_{nlm}(\zeta,r) = \frac{(2\zeta)^{n+1/2}}{\sqrt{(2n)!}} r^{n-1}[\exp(-\zeta r)]Y_{lm}(\vartheta,\varphi) \qquad (A.1)$$

typically serve as efficient basis sets in semiempirical molecular orbital theories, e.g. extended Hückel (EH) calculations. A serious complication arises whenever an atom's effective potential within a molecule deviates substantially from the original atomic potential. Then the ζ orbital exponent, determined by the effective nuclear charge, needs modification. This perturbative effect is clearly most prominent for alkali metal atoms, having only one electron in the valence s level.

To minimize this error source and strive for the highest possible calculational reliability, we therefore optimized in a stepwise manner the Li-2s, Li-2p, Al-3s, and Al-3p orbital exponents, for both α- and γ-$LiAlO_2$, starting from Fitzpatrick's consistent set of ζ values[57] which were determined by fitting Slater orbitals to numerical Herman–Skillman functions.

The optimization was performed as follows. First the total energies E^0 were calculated for at least four different Li-2s exponents. The resulting E^0–ζ curve was interpolated by a polynomial of third order (goodness of fit ≥ 0.999) whose minimum was determined analytically. Setting ζ of Li-2s to this new value, the next exponent (Li-2p, then Al-3s, finally Al-3p) was refined as described before. O orbital exponents were not touched, and α- and γ-$LiAlO_2$ were treated separately.

The observed E^0–ζ curves for Li and Al are presented in Figures 11 and 12, respectively. Surprisingly (see discussion below), the refinement was straightforward, and we encountered no saddle points. As expected, the E^0–ζ dependence is strongest for the Li–2s level (highest filled atomic orbital) and smallest for the Al–3s level (lowest filled atomic orbital). Interestingly, Li-2p exponents refine to the same numerical value in both modifications, and approximately the same holds for Al-3p. The Li atom is slightly more contracted in γ-$LiAlO_2$ than in α-$LiAlO_2$. A larger difference is only found for Al-3s, where this orbital turns out to be smaller in the γ-modification. In order to maximize the overlap population with neighboring O atoms and thus to lower the total energy, the geometrical constraints of the O tetrahedron (γ, *short* Al–O distances) and of the O octahedron (α, *long* Al–O distances), determining the size of the overlap integral S_{ij} between Al-3s and O-2s, favor the doubly filled 3s orbital to be more contracted within an O tetrahedron than within an O octahedron.

We have to admit, of course, that the above refinement procedure cannot be rigorously justified for a nonvariational method such as EH theory. Our approach should be understood as a way of maximizing chemical bonding in $LiAlO_2$. However, the refinement being completed,

(57) Fitzpatrick, N. J.; Murphy, G. H. *Inorg. Chim. Acta* **1984**, *87*, 41.

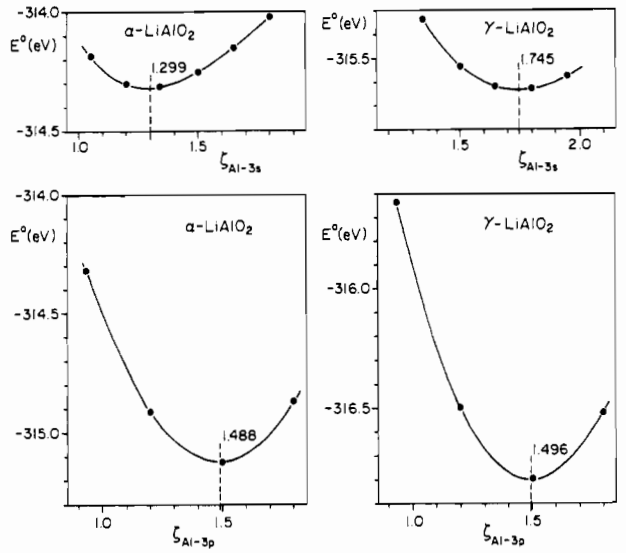

Figure 12. Refinement of the Al-3s (top) and Al-3p (bottom) Slater-type orbital exponents ζ within α-$LiAlO_2$ (left) and γ-$LiAlO_2$ (right). The exponent values leading to the lowest total energies E_0 (eV) are indicated by dashed lines.

all gross Mulliken charges of Li, Al, and O atoms are significantly smaller than those charges (in parentheses) that were computed using Fitzpatrick's exponents:

$q^{\alpha}_{Li} = 0.444\ (0.507)$ $q^{\gamma}_{Li} = 0.261\ (0.550)$
$q^{\alpha}_{Al} = 2.111\ (2.520)$ $q^{\gamma}_{Al} = 1.884\ (2.305)$
$q^{\alpha}_{O} = -1.278\ (-1.514)$ $q^{\gamma}_{O} = -1.072\ (-1.428)$

Thus, another possible serious error related to EH theory (from implicitly neglecting electrostatic effects) is reduced as well, and the optimization technique has found an a posteriori justification.

Appendix B. Core Repulsion Energy

By neglecting core repulsion energies, extended Hückel (EH) theory usually does not yield reliable potential energy curves for stretching motions. For example, an EH optimum Li–O bond length would approximately equal the distance where the Li-2s–O-2p overlap integral is maximized (using Fitzpatrick's exponents[57] at about 32 pm), too short by 115 pm if compared to a Li–O single-bond length.[34]

However, much better potential energy curves can easily be obtained by introducing additional two-body repulsive terms[49,58] as done by Anderson and Hoffmann as well as by Calzaferri and co-workers. One can also augment the minimal basis set with inner shells,[59] which probably is the physically more transparent technique. Of course, there are no *additional* quantum-mechanical repulsive interactions while atomic pairs are contracted below their equilibrium distance—it is simply the Pauli principle at work which makes the bond more stiff.

We decided to include the inner 1s level of Li to achieve more reasonable activation barriers in pushing the Li atom through the small O triangles. To obtain a rough energy estimate of all one-electron eigenvalues, a quick atomic energy calculation with the modified[60] code of Desclaux[61] gave the following Hartree–Fock–Slater eigenvalues[62] for the Li atom (values for Li^+ ion in parentheses):

$$\mathcal{E}_{1s} = -52.99\ \text{eV}\ (-69.05\ \text{eV})$$
$$\mathcal{E}_{2s} = -5.34\ \text{eV}\ (-15.14\ \text{eV})$$
$$\mathcal{E}_{2p} = -3.49\ \text{eV}\ (-13.63\ \text{eV})$$

The energy gap between 1s and 2s levels equals about 48 eV (54 eV) for the Li atom (Li^+ ion). Since the chemical binding within $LiAlO_2$ is mainly ionic, the 1s level was fixed 54 eV below the 2s level, at –63 eV. With the assumption of cyclic boundary conditions (infinite crystal), having no contact to the vacuum level, the *absolute* levels in energy are perfectly arbitrary. The ζ exponent of Li-1s was taken from Fitzpatrick.[57]

As a result, the total energies of α-$LiAlO_2$ and γ-$LiAlO_2$ are –314.58 and –316.12 eV, weakened by 0.55 and 0.68 eV if compared to the preceding calculations without core levels. Thus, core repulsion diminishes the *cohesive* energies (total binding energies), even at the equilibrium distance, by roughly 2.0 and 2.3% for the α- and γ-modifications, respectively. The new energy difference between both modifications is 1.54 eV, about 8% lower than the one without core repulsion. So the quantitative difference between α- and γ-$LiAlO_2$ remains nearly unchanged.

(58) Calzaferri, G.; Forss, L.; Kamber, I. *J. Phys. Chem.* **1989**, *93*, 5366.
(59) Künne, L. D. *Monatsh. Chem.* **1991**, *122*, 625.
(60) Klobukowski, M. *Comput. Phys. Commun.* **1982**, *25*, 29.
(61) Desclaux, J. P. *Comput. Phys. Commun.* **1969**, *1*, 216.
(62) The $X\alpha$ parameter for the approximate treatment of the nonlocal exchange potential,[63] highly *insensitive* for different ionicities,[64] was set to 0.781. All spin–orbit and relativistic corrections were neglected.
(63) Slater, J. C. *Phys. Rev.* **1951**, *81*, 385.
(64) Schwarz, K. *Phys. Rev. B* **1972**, *5*, 2466.